

## Multigrid Formulation of Polynomial Flux-Difference Splitting for Steady Euler Equations

ERIK DICK

*Department of Machinery, State University of Ghent,  
Sint Pietersnieuwstraat 41, B-9000 Ghent, Belgium*

Received March 31, 1989; revised October 11, 1989

A flux-difference splitting method based on the polynomial character of the flux vectors is applied to steady Euler equations. The discretization is done with a vertex-centered finite volume method. In first-order form, a discrete set of equations is obtained which is both conservative and positive. The flux-difference splitting is done in an algebraically exact way, so that shocks are represented without wiggles. Due to the positivity, the set of equations can be solved by collective relaxation methods. A full multigrid method based on symmetric successive relaxation, full weighting, bilinear interpolation and  $W$ -cycle is presented. In first-order form, typical full multigrid efficiency is achieved. This is demonstrated on the GAMM transonic bump test-case. The second-order formulation is based on the Roe–Chakravarthy minmod-limiter. The discrete system is solved using a multigrid defect-correction formulation. The second-order formulation is demonstrated on Harten's shock reflection problem. © 1990 Academic Press, Inc.

### 1. INTRODUCTION

A flux-difference splitting method based on the polynomial character of the flux-vectors was introduced by the author in [1]. This splitter has properties which are similar to the splitter introduced by Roe [2]. In contrast to Roe's splitter, which is based on the quadratic character of the flux-vectors with respect to the variables  $\sqrt{\rho}$ ,  $\sqrt{\rho} u$ ,  $\sqrt{\rho} v$ ,  $\sqrt{\rho} H$ , the splitter relies only on the polynomial character with respect to the primitive variables  $\rho$ ,  $u$ ,  $v$ ,  $p$ , avoiding in this way square root evaluations. The polynomial splitter was inspired by earlier work by Lombard *et al.* [3], where the same idea was used in an approximate way. An algebraically exact formulation, however, is necessary to arrive at discrete equations which can be solved by relaxation methods.

Multigrid formulations using this technique, with first order accuracy were presented by the author in [4, 5]. In this paper, the principles of the splitting are briefly reviewed and the multigrid formulation in first order form and second order form, using defect correction, is discussed.

## 2. POLYNOMIAL FLUX-DIFFERENCE SPLITTING

Steady Euler equations, in two dimensions, take the form

$$\frac{\partial f}{\partial x} + \frac{\partial g}{\partial y} = 0, \quad (1)$$

where the flux-vectors are

$$\begin{aligned} f^T &= \{\rho u, \rho u u + p, \rho u v, \rho H u\}, \\ g^T &= \{\rho v, \rho u v, \rho v v + p, \rho H v\}; \end{aligned} \quad (2)$$

$\rho$  is density,  $u$  and  $v$  are Cartesian velocity components,  $p$  is pressure,  $H = \gamma p / (\gamma - 1) \rho + \frac{1}{2} u^2 + \frac{1}{2} v^2$  is total enthalpy and  $\gamma$  is the adiabatic constant. Since the components of the flux-vectors form polynomials with respect to the primitive variables  $\rho$ ,  $u$ ,  $v$ , and  $p$ , components of flux-differences can be written as

$$\begin{aligned} \Delta \rho u &= \bar{u} \Delta \rho + \bar{\rho} \Delta u, \\ \Delta(\rho u u + p) &= \bar{\rho} \bar{u} \Delta u + \bar{u} \Delta \rho u + \Delta p \\ &= \bar{u}^2 \Delta \rho + (\bar{\rho} \bar{u} + \bar{\rho} \bar{u}) \Delta u + \Delta p, \\ \Delta \rho H u &= \bar{\rho} \bar{u} \left( \frac{1}{2} \Delta u^2 + \frac{1}{2} \Delta v^2 \right) + \frac{1}{2} (\bar{u}^2 + \bar{v}^2) \Delta \rho u + \frac{\gamma}{\gamma - 1} \Delta p u \\ &= \frac{1}{2} (\bar{u}^2 + \bar{v}^2) \bar{u} \Delta \rho + \frac{1}{2} (\bar{u}^2 + \bar{v}^2) \bar{\rho} \Delta u + \bar{\rho} \bar{u} \bar{u} \Delta u \\ &\quad + \frac{\gamma}{\gamma - 1} \bar{p} \Delta u + \bar{\rho} \bar{u} \bar{v} \Delta v + \frac{\gamma}{\gamma - 1} \bar{u} \Delta p, \end{aligned}$$

etc., where the bar denotes mean value.

With the definition of  $\bar{q} = \frac{1}{2}(\bar{u}^2 + \bar{v}^2)$ , the flux-difference  $\Delta f$  can be written as

$$\Delta f = \begin{pmatrix} \bar{u} & \bar{\rho} & 0 & 0 \\ \bar{u}^2 & \bar{\rho} \bar{u} + \bar{\rho} \bar{u} & 0 & 1 \\ \bar{u} \bar{v} & \bar{\rho} \bar{v} & \bar{\rho} \bar{u} & 0 \\ \bar{q} \bar{u} & \bar{q} \bar{\rho} + \bar{\rho} \bar{u} \bar{u} + \frac{\gamma}{\gamma - 1} \bar{p} & \bar{\rho} \bar{u} \bar{v} & \frac{\gamma}{\gamma - 1} \bar{u} \end{pmatrix} \Delta \xi,$$

where  $\xi^T = \{\rho, u, v, p\}$ .

With the definition of  $\bar{u}$  by  $\bar{\rho} \bar{u} = \bar{\rho} \bar{u}$ , the flux-difference  $\Delta f$  is given by

$$\Delta f = \begin{pmatrix} 1 & 0 & 0 & 0 \\ \bar{u} & \bar{\rho} & 0 & 0 \\ \bar{v} & 0 & \bar{\rho} & 0 \\ \bar{q} & \bar{\rho} \bar{u} & \bar{\rho} \bar{v} & 1/\gamma - 1 \end{pmatrix} \begin{pmatrix} \bar{u} & \bar{\rho} & 0 & 0 \\ 0 & \bar{u} & 0 & 1/\bar{\rho} \\ 0 & 0 & \bar{u} & 0 \\ 0 & \gamma \bar{p} & 0 & \bar{u} \end{pmatrix} \Delta \xi. \quad (3)$$

By denoting the first matrix in (3) by  $T$ , it is easily seen that the flux-difference  $\Delta g$  can be written in a similar way as

$$\Delta g = T \begin{pmatrix} \bar{v} & 0 & \bar{\rho} & 0 \\ 0 & \bar{\bar{v}} & 0 & 0 \\ 0 & 0 & \bar{v} & 1/\bar{\rho} \\ 0 & 0 & \gamma\bar{\rho} & \bar{v} \end{pmatrix} \Delta \xi, \quad (4)$$

where  $\bar{\rho}\bar{\bar{v}} = \bar{\rho}\bar{v}$ .

Any linear combination of  $\Delta f$  and  $\Delta g$  can be written as

$$\Delta \phi = n_x \Delta f + n_y \Delta g = A \Delta \xi = T \tilde{A} \Delta \xi, \quad (5)$$

where

$$\tilde{A} = \begin{pmatrix} \bar{w} & n_x \bar{\rho} & n_y \bar{\rho} & 0 \\ 0 & \bar{\bar{w}} & 0 & n_x / \bar{\rho} \\ 0 & 0 & \bar{\bar{w}} & n_y / \bar{\rho} \\ 0 & n_x \gamma \bar{\rho} & n_y \gamma \bar{\rho} & \bar{w} \end{pmatrix}, \quad (6)$$

with  $\bar{w} = n_x \bar{u} + n_y \bar{v}$ ,  $\bar{\bar{w}} = n_x \bar{\bar{u}} + n_y \bar{\bar{v}}$ .

It is easy to verify that the matrix  $\tilde{A}$  has real eigenvalues and a complete set of eigenvectors [1]. For  $n_x^2 + n_y^2 = 1$ , the eigenvalues are given by

$$\lambda_1 = \bar{w}, \quad \lambda_2 = \bar{\bar{w}}, \quad \lambda_3 = \bar{w} + \bar{c}, \quad \lambda_4 = \bar{w} - \bar{c},$$

where

$$\bar{w} = (\bar{w} + \bar{\bar{w}})/2 \quad \text{and} \quad \bar{c}^2 = \gamma \bar{\rho} / \bar{\rho} + (\bar{w} - \bar{\bar{w}})^2 / 4.$$

Following the procedure of Steger and Warming [6], the matrix  $\tilde{A}$  can be split into positive and negative parts by

$$\tilde{A}^+ = R A^+ L, \quad \tilde{A}^- = R A^- L, \quad (7)$$

where  $R$  and  $L$  denote right and left eigenvector matrices, in orthonormal form and where

$$A^+ = \text{diag}(\lambda_1^+, \lambda_2^+, \lambda_3^+, \lambda_4^+), \quad A^- = \text{diag}(\lambda_1^-, \lambda_2^-, \lambda_3^-, \lambda_4^-),$$

with  $\lambda_i^+ = \max(\lambda_i, 0)$ ,  $\lambda_i^- = \min(\lambda_i, 0)$ .

With positive and negative matrices, matrices with respectively non-negative and non-positive eigenvalues are meant. This allows a splitting of the flux-difference (5) by

$$\Delta \phi = A^+ \Delta \xi + A^- \Delta \xi, \quad (8)$$

with  $A^+ = T \tilde{A}^+$ ,  $A^- = T \tilde{A}^-$ .

In order to justify (8), it is important to remark that the matrix  $T$  is the discrete analogue of the similarity transformation matrix between conservative and primitive variables. Indeed, one verifies that

$$T \Delta \xi = \Delta \zeta,$$

where  $\zeta^T = (\rho, \rho u, \rho v, \rho E)$ , with total energy  $E = p/(\gamma - 1)\rho + \frac{1}{2}u^2 + \frac{1}{2}v^2$ . Hence

$$\Delta \phi = A \Delta \xi = T \tilde{A} \Delta \xi = T \tilde{A} T^{-1} \Delta \zeta = TRALT^{-1} \Delta \zeta = TRAL \Delta \xi. \quad (9)$$

As a consequence, a splitting of  $\tilde{A}$  results in a splitting of  $A$ .

### 3. CONSTRUCTION OF A POSITIVE DISCRETIZATION

Figure 1 shows the control volume centered around the node  $(i, j)$ . With piecewise constant interpolation of variables, the flux-difference over the surface  $S_{i+1/2}$  of the control volume can be written as

$$\begin{aligned} \Delta F_{i,i+1} &= \Delta y_{i+1/2} \Delta f_{i,i+1} + \Delta x_{i+1/2} \Delta g_{i,i+1} \\ &= \Delta s_{i+1/2} (n_x \Delta f_{i,i+1} + n_y \Delta g_{i,i+1}), \end{aligned} \quad (10)$$

where  $\Delta s_{i+1/2}^2 = \Delta x_{i+1/2}^2 + \Delta y_{i+1/2}^2$ ,  $n_x = \Delta y_{i+1/2} / \Delta s_{i+1/2}$ ,  $n_y = \Delta x_{i+1/2} / \Delta s_{i+1/2}$ ;  $n_x$  and  $n_y$  denote the components of the unit outgoing normal to the control surface.

With the notation of the previous section, the flux-difference is

$$\Delta F_{i,i+1} = F_{i+1} - F_i = \Delta s_{i+1/2} A_{i,i+1} \Delta \xi_{i,i+1}. \quad (11)$$

Furthermore, the matrix  $A_{i,i+1}$  can be split into positive and negative parts. This allows the definition of the absolute value of the flux-difference by

$$|\Delta F_{i,i+1}| = \Delta s_{i+1/2} (A_{i,i+1}^+ - A_{i,i+1}^-) \Delta \xi_{i,i+1}. \quad (12)$$

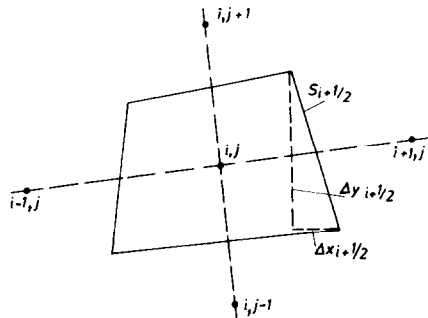


FIG. 1. Vertex-centered finite volume formulation.

Based on (12) an upwind definition of the flux is

$$F_{i+1/2} = \frac{1}{2}[F_i + F_{i+1} - |\Delta F_{i,i+1}|]. \quad (13)$$

That this represents an upwind flux can be verified by writing (13) in either of the two following ways, which are completely equivalent:

$$\begin{aligned} F_{i+1/2} &= F_i + \frac{1}{2} \Delta F_{i,i+1} - \frac{1}{2} |\Delta F_{i,i+1}| \\ &= F_i + \Delta s_{i+1/2} A_{i,i+1}^- \Delta \xi_{i,i+1}, \end{aligned} \quad (14)$$

$$\begin{aligned} F_{i+1/2} &= F_{i+1} - \frac{1}{2} \Delta F_{i,i+1} - \frac{1}{2} |\Delta F_{i,i+1}| \\ &= F_{i+1} - \Delta s_{i+1/2} A_{i,i+1}^+ \Delta \xi_{i,i+1}. \end{aligned} \quad (15)$$

Indeed, when  $A_{i,i+1}$  only has positive eigenvalues, the flux  $F_{i+1/2}$  is taken to be  $F_i$  and when  $A_{i,i+1}$  only has negative eigenvalues, the flux  $F_{i+1/2}$  is taken to be  $F_{i+1}$ .

The fluxes on the other surfaces of the control volume  $S_{i-1/2}$ ,  $S_{j+1/2}$ ,  $S_{j-1/2}$ , can be treated in a similar way. With (14) and (15), the flux balance on the control volume of Fig. 1 has the form

$$\begin{aligned} \Delta s_{i+1/2} A_{i,i+1}^- [\xi_{i+1} - \xi_i] + \Delta s_{i-1/2} A_{i,i-1}^+ [\xi_i - \xi_{i-1}] \\ + \Delta s_{j+1/2} A_{j,j+1}^- [\xi_{j+1} - \xi_j] + \Delta s_{j-1/2} A_{j,j-1}^+ [\xi_j - \xi_{j-1}] = 0. \end{aligned} \quad (16)$$

The set formed by Eq. (16) for all nodes is a so-called positive set. This can be seen by writing (16) as

$$\begin{aligned} C \xi_{i,j} &= \Delta s_{i-1/2} A_{i,i-1}^+ \xi_{i-1} + \Delta s_{i+1/2} (-A_{i,i+1}^-) \xi_{i+1} \\ &+ \Delta s_{j-1/2} A_{j,j-1}^+ \xi_{j-1} + \Delta s_{j+1/2} (-A_{j,j+1}^-) \xi_{j+1}, \end{aligned} \quad (17)$$

where  $C$  is the sum of the matrix-coefficients in the right-hand side and where these coefficients have non-negative eigenvalues.

As a consequence of the positivity, a solution can be obtained by a collective variant of any scalar relaxation method. By a collective variant it is meant that, in each node, all components of the vector of dependent variables  $\xi$  are relaxed simultaneously.

In practise, the flux-balance (16) is formed by summing expressions of type (14) over all surfaces, using the appropriate components of the unit outgoing normal  $n_x$  and  $n_y$  in the definition of the Jacobian (6).

#### 4. BOUNDARY CONDITIONS

Figure 2 shows the half-volume centered around a node on a solid boundary. This half-volume can be seen as the limit of a complete volume in which one of

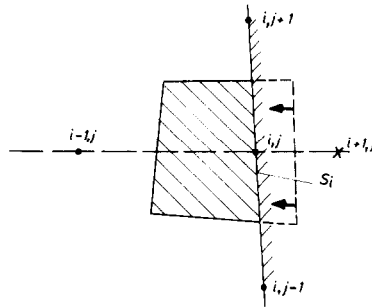


FIG. 2. Treatment of boundary conditions.

the sides tends to the boundary. As a consequence, the flux on the side  $S_i$  of the boundary control volume can be expressed according to (14) by

$$F_i + \Delta s_i A_{i,j}^- (\xi_{i+1} - \xi_i), \quad (18)$$

where the matrix  $A_{i,j}^-$  is calculated in the node  $(i, j)$ .

With the definition (18), the flux balance on the control volume at the boundary takes the form (16) in which a node outside the domain comes in. This node, however, can be eliminated. On a solid boundary, two eigenvalues of the matrix  $\tilde{A}_{i,j}$  are zero due to the boundary condition of tangentiality:

$$\lambda_1 = \bar{w} = 0, \quad \lambda_2 = \bar{v} = 0.$$

The third and the fourth eigenvalues are given by

$$\lambda_3 = \bar{c}, \quad \lambda_4 = -\bar{c}.$$

As a consequence, the rank of the matrix  $A_{i,j}^-$  is equal to one. This means that premultiplication of the flux-balance on a solid boundary by  $l_{i,j} T_{i,j}^{-1}$ , where  $l_{i,j}$  is a left eigenvector associated to a zero eigenvalue of  $\tilde{A}_{i,j}^-$ , yields an equation where the outside node is eliminated. This results in three equations. These are to be supplemented by the boundary condition of tangentiality. A similar procedure can be used at inflow and at outflow. At subsonic inflow, (18) yields one equation that requires three additional relations to be prescribed by the boundary conditions. At subsonic outflow, (18) yields three equations and one boundary condition is to be given. Physically, as inlet boundary conditions, stagnation pressure, stagnation temperature, and flow direction are to be prescribed. At outlet, the Mach number can be prescribed. Explicit expressions of the combinations of the equations at boundaries are given in [1].

Due to the linearity of the condition of impermeability, the set of equations on a solid boundary is a quasi-linear set which is similar to the set in the flow field. At inflow and outflow boundaries, the physical boundary conditions are highly non-linear combinations of the primitive variables. Therefore, the introduction of

the boundary conditions at inlet and outlet, in the way described above, necessitates iteration. This complicates the algorithm. Therefore, it is better to treat the nodes at inlet and outlet as auxiliary points and to determine the variables in these points by extrapolation. At inlet, Mach number is extrapolated along streamlines. Together with the given boundary conditions, this determines all flow variables in a direct way. At outflow the stagnation values and the flow direction are extrapolated along streamlines. Together with the prescribed Mach number, again this determines all flow variables in a direct way.

### 5. MULTIGRID FORMULATION FOR A TRANSONIC APPLICATION

Figure 3 shows the well-known GAMM-test case [7] for transonic flows, discretized by a grid with  $24 \times 8$  elements. This grid is the third in a series of four. The finest grid has  $96 \times 32$  elements. Vertex-centered finite volumes, as indicated in Fig. 2, were used. At inflow, the specification of a horizontal flow direction was used as boundary condition. At outflow, the Mach number was fixed at 0.85.

Figure 4 shows the iso-Mach lines for the fully converged solution plotted by piecewise linear interpolation within the elements of the grid. The obtained solution almost coincides with the solutions obtained from the most reliable time-marching methods reported in [7]. However, unlike most time-marching solutions, due to the guaranteed positivity, the solution has no wiggles in the shock region.

Figure 5 shows the cycle-structure of the multigrid method. Both the starting cycle and the repeated cycle have  $W$ -form. A full approximation scheme (FAS) on the non-linear equations (17) is used. The relaxation algorithm is symmetric Gauss-Seidel. The order of relaxation is the lexicographic order, i.e., going from the lower left point to the upper right point, first varying the row index, and then going from the upper right point to the lower left point in the reverse order. In relaxing the set of Eq. (17), the coefficients are formed with the latest available information. This means that in the first sweep  $A_{i,i-1}^+$  is evaluated with the function values in

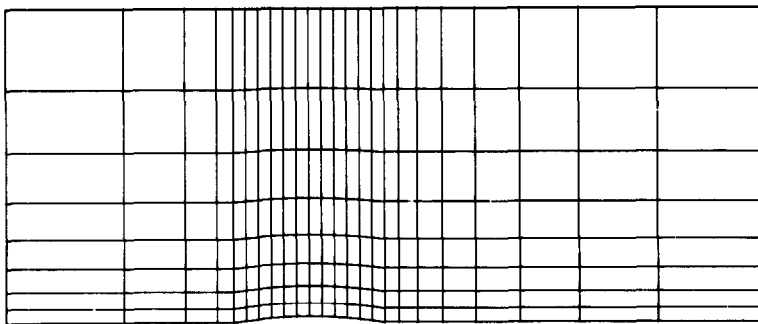


FIG. 3. The GAMM-test case for transonic flows, discretized with a  $24 \times 8$  grid.

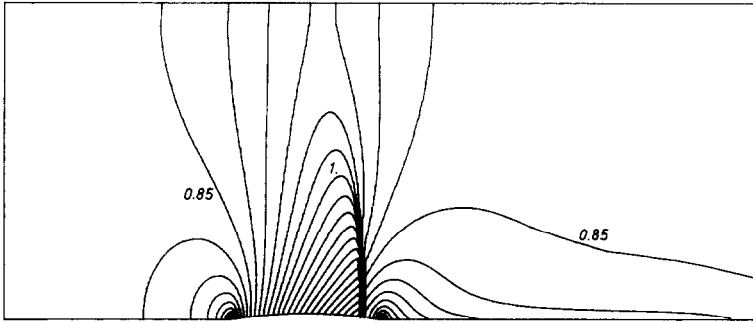


FIG. 4. Iso-Mach lines for the testcase of Fig. 3 on the  $96 \times 32$  grid.

node  $(i, j)$  on the new level. After determination of the new values in node  $(i, j)$ , no updates of coefficients and no extra iterations are done. This means that the set of Eq. (17) is treated as a quasi-linear set. As restriction operator for residuals, full weighting is used within the flow field while injection is used at the boundaries. The prolongation operator is bilinear interpolation. The restriction for function values is injection. The calculation starts from a uniform flow with Mach number 0.85 on the coarsest grid ( $12 \times 4$ ).

The multigrid procedure for the first-order formulation used here is very similar to the one formulated by Hemker and Spekrijse [8]. The differences with this earlier work are that here a vertex-centered formulation is used instead of a cell-centered formulation and that the polynomial flux-difference splitting with respect to primitive variables is used instead of the Osher-splitting [9] with respect to entropy variables.

In Fig. 5, the operation count is indicated. A relaxation on the current grid is taken as one local work unit. So, the symmetric relaxation is seen as two work units. A residual evaluation plus the associated grid transfer is also taken as one local work unit. Hence, the 4 in Fig. 5, in going down, stands for the construction of the right-hand side in the FAS-formulation, two relaxations, and one residual evaluation. With this way of evaluating the work, the cost of the repeated cycle is 9.4375 work units on the finest level. The cost of the starting cycle is 5.1875 work units.

Figure 6 shows the convergence behaviour of the single grid and the multigrid

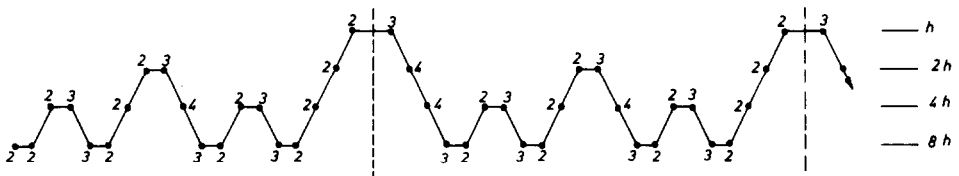


FIG. 5. Cycle-structure of the multigrid method.



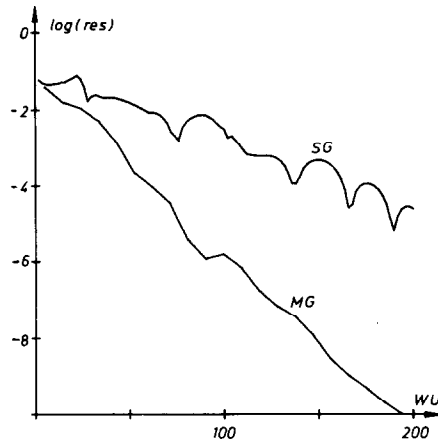


FIG. 6. Convergence history of single grid and multigrid formulation for the transonic test case.

formulation. The residual shown is the maximum residual of all equations, after normalizing these equations, i.e., setting the coefficient of  $\rho$ ,  $u$ ,  $v$ , and  $p$  on 1 in the mass, momentum- $x$ , momentum- $y$ , and energy equations, respectively, and dividing the variables by their value in the initial uniform flow.

The convergence factor of the multigrid method, i.e., the residual reduction per work unit is about 0.895 or about 0.355 per cycle. This can be considered as being optimal.

## 6. SECOND-ORDER FORMULATION

Figure 7 shows Harten's well-known shock reflection problem, together with the first-order solution obtained by the previous method, using a rectangular  $96 \times 32$

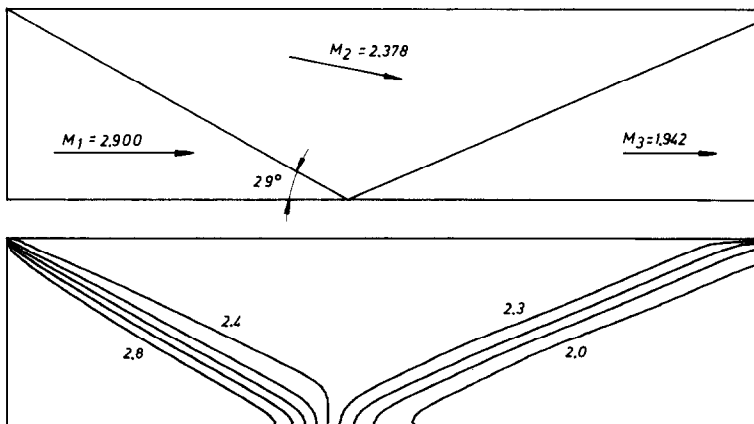


FIG. 7. Harten's shock reflection problem with iso-Mach lines of the first-order solution for a  $96 \times 32$  grid.

elements grid. The smoothing of the oblique shocks is evident. In order to obtain second-order accuracy, the definition of the flux (13) is modified.

First, we remark that, using (9), the flux-difference (11) can be written as

$$\Delta F_{i,i+1} = \Delta s_{i+1/2} \sum_n T_{i+1/2} r_{i+1/2}^n \lambda_{i+1/2}^n l_{i+1/2}^n \Delta \xi_{i,i+1}, \quad (19)$$

where the superscript  $n$  refers to the  $n$ th eigenvalue and where  $r^n$  and  $l^n$  denote the  $n$ th right and left eigenvectors.

By denoting the projection of  $\Delta \xi_{i,i+1}$  on the  $n$ th eigenvector by

$$\sigma_{i+1/2}^n = l_{i+1/2}^n \Delta \xi_{i,i+1}$$

and using

$$\tilde{r}_{i+1/2}^n = T_{i+1/2} r_{i+1/2}^n,$$

(19) can be written as

$$\begin{aligned} \Delta F_{i,i+1} &= \sum_n \Delta F_{i,i+1}^n = \Delta s_{i+1/2} \sum_n \tilde{r}_{i+1/2}^n \lambda_{i+1/2}^n \sigma_{i+1/2}^n \\ &= \sum_n \tilde{r}_{i+1/2}^n \tau_{i+1/2}^n, \end{aligned} \quad (20)$$

where  $\Delta F_{i,i+1}^n$  denotes the component of the flux-difference associated to the  $n$ th eigenvalue and  $\tau_{i+1/2}^n$  is the projection of the flux-difference on the  $n$ th eigenvector.

Using (20), the first-order flux (13) can be written as

$$F_{i+1/2} = \frac{1}{2} (F_i + F_{i+1}) - \frac{1}{2} \sum_n \Delta F_{i,i+1}^{n+} + \frac{1}{2} \sum_n \Delta F_{i,i+1}^{n-}, \quad (21)$$

where the  $+$  and  $-$  superscripts denote the positive and negative parts of the components of the flux-difference, i.e., the parts obtained by taking the positive and negative parts of the eigenvalues.

According to Chakravarthy and Osher [10], a second-order flux corresponding to (21) can be defined by

$$\begin{aligned} F_{i+1/2} &= \frac{1}{2} (F_i + F_{i+1}) - \frac{1}{2} \sum_n \Delta F_{i,i+1}^{n+} + \frac{1}{2} \sum_n \Delta F_{i,i+1}^{n-} \\ &\quad + \frac{1}{2} \sum_n \tilde{\Delta F}_{i-1,i}^{n+} - \frac{1}{2} \sum_n \tilde{\Delta F}_{i+1,i+2}^{n-}, \end{aligned} \quad (22)$$

where

$$\begin{aligned} \tilde{\Delta F}_{i-1,i}^{n+} &= \Delta s_{i+1/2} \tilde{r}_{i+1/2}^n \lambda_{i-1/2}^n l_{i+1/2}^n \Delta \xi_{i-1,i} \\ &= \tilde{r}_{i+1/2}^n \tau_{i-1/2}^n, \end{aligned} \quad (23)$$

with a similar definition for  $\tilde{\Delta F}_{i+1,i+2}^{n-}$ .

Clearly (23) is constructed by considering a flux-difference over the surface  $S_{i+1/2}$ , i.e., using the geometry of this surface, with data shifted in the negative  $i$ -direction.  $\tau_{i-1/2}^n$  represents the projection of this flux-difference on the  $n$ th eigenvector of the unshifted flux-difference.

Definition (22) corresponds to a second-order upwind flux. This easily can be seen by considering the case where all eigenvalues have the same sign. Second-order accuracy also can be reached by taking a central definition of the flux vector:

$$\bar{F}_{i+1/2} = \frac{1}{2}(F_i + F_{i+1}). \quad (24)$$

As is well known, using either (22) or (24) leads to a scheme which is not monotonicity preserving so that wiggles in the solution become possible. Following the theory of the flux limiters [11], a combination of (22) and (24) is taken. This takes the form

$$\begin{aligned} F_{i+1/2} = & \frac{1}{2}(F_i + F_{i+1}) - \frac{1}{2} \sum_n \Delta F_{i,i+1}^{n+} + \frac{1}{2} \sum_n \Delta F_{i,i+1}^{n-} \\ & + \frac{1}{2} \sum_n \tilde{\Delta} F_{i-1,i}^{n+} - \frac{1}{2} \sum_n \tilde{\Delta} F_{i+1,i+2}^{n-}, \end{aligned} \quad (25)$$

with

$$\tilde{\Delta} F_{i-1,i}^{n+} = \text{Lim}(\tilde{\Delta} F_{i-1,i}^{n+}, \Delta F_{i,i+1}^{n+}), \quad (26)$$

$$\tilde{\Delta} F_{i+1,i+2}^{n-} = \text{Lim}(\tilde{\Delta} F_{i+1,i+2}^{n-}, \Delta F_{i,i+1}^{n-}), \quad (27)$$

where Lim denotes some limited combination of both arguments. We choose here the simplest possible form of a limiter, i.e.,

$$\text{Lim} = \text{MinMod},$$

where the function MinMod returns the arguments with minimum absolute value if both arguments have the same sign and returns zero otherwise. By the use of the limiter to the vectors (26), (27) it is meant that the limiter is used component-wise, i.e., applied to the  $\tau$ -values.

At boundaries and in the vicinity of boundaries, some of the flux-differences in (26) or (27) do not exist. In this case, the limiter returns a zero. This does not cause a degradation of the second-order accuracy at boundaries, since due to the construction of the boundary equations no information is taken from nodes outside the flow field.

Figure 8 shows the solution obtained with the second-order formulation for Harten's shock reflection problem. Since for the discretization obtained by the second-order formulation, the positivity is not guaranteed, a relaxation method on this formulation is impossible. Therefore as a solution procedure a defect-correction

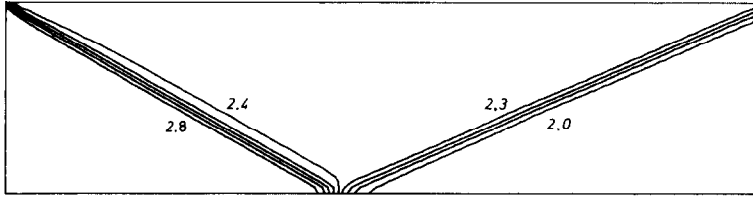


FIG. 8. Iso-Mach lines for the second-order solution of Harten's shock reflection problem.

formulation was used. By denoting symbolically the first-order and second-order formulation on the finest grid by

$$L_h^1 = r_h^1, \quad (28)$$

$$L_h^2 = r_h^2, \quad (29)$$

a defect correction means that (28) is replaced by

$$L_h^1 = r_h^1 + [(L_h^1 - r_h^1) - (L_h^2 - r_h^2)], \quad (30)$$

where  $L$  and  $r$  indicate left- and right-hand sides.

In (30) the difference of the defects of the first- and second-order discretization is added to the right-hand side. The defect-correction is only performed on the finest grid so that the multigrid formulation of the first-order discretization still can be used. For a principal description of the defect-correction approach, the reader is referred to [12] and for the application to steady Euler equations to [13].

Figure 9 shows the convergence behaviour of the first- and second-order multigrid methods. The defect-correction was used from the first cycle. The calculation

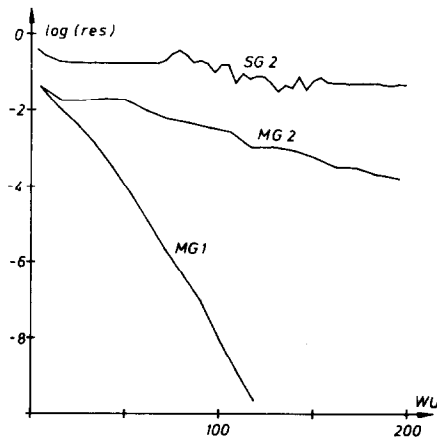


FIG. 9. Convergence history of first- and second-order multigrid formulation, compared with second-order single grid formulation for Harten's shock reflection problem.

starts from a uniform flow with Mach number 2.9 on the coarsest grid. In calculating the work units in Fig. 9, the work involved in the calculation of the difference of the defects was taken to be 1.75 work units. This amount of work was determined from actual computing times. The residual reduction in the first-order formulation is 0.220 per cycle (=9.4375 work units). For the second-order formulation it degrades to about 0.720 per cycle. This efficiency loss is comparable to the loss suffered by Koren and Spekreijse [14] with a similar defect-correction formulation, however, using a completely different splitting and a completely different limiter.

For reasons of comparison, in Fig. 9, also the single grid performance, using defect correction is indicated. One defect-correction is done for each symmetric relaxation so that the work spent in a single grid operation is 3.75 work units.

## 7. CONCLUSION

It has been shown that, by the use of an adequate flux-difference splitting technique, a multigrid method can be obtained for steady Euler equations. The usual multigrid performance is obtained.

## REFERENCES

1. E. DICK, *J. Comput. Phys.* **76**, 19 (1988).
2. P. L. ROE, *J. Comput. Phys.* **43**, 357 (1981).
3. C. K. LOMBARD, J. OLIGER, AND J. Y. YANG, AIAA paper 82-0976, 1982.
4. E. DICK, in *Lecture Notes in Physics*, Vol. 323, edited by D. L. Dwoyer, M. Y. Hussaini, and R. G. Voigt (Springer-Verlag, Berlin, 1989), p. 225.
5. E. DICK, *J. Comput. Appl. Math.* **28**, 173 (1989).
6. J. L. STEGER AND R. F. WARMING, *J. Comput. Phys.* **40**, 263 (1981).
7. *Notes on Numerical Fluid Dynamics* 3, edited by A. Rizzi and H. Viviand (Vieweg, Braunschweig, 1981).
8. P. W. HEMKER AND S. P. SPEKREIJSE, *Appl. Numer. Math.* **2**, 475 (1986).
9. S. OSHER AND S. R. CHAKRAVARTHY, *J. Comput. Phys.* **50**, 447 (1983).
10. S. R. CHAKRAVARTHY AND S. OSHER, AIAA paper 85-0363, 1985.
11. P. K. SWEBY, *SIAM J. Numer. Anal.* **21**, 995 (1984).
12. K. BÖHMER, P. W. HEMKER, AND H. J. STETTER, *Comput. Suppl.* **5**, 1 (1984).
13. P. W. HEMKER, in *Lecture Notes in Mathematics*, Vol. 1228, edited by W. Hackbusch and U. Trottenberg (Springer-Verlag, Berlin, 1986), p. 149.
14. B. KOREN AND S. SPEKREIJSE, in *Lecture Notes in Pure and Applied Mathematics*, Vol. 110, edited by S. F. McCormick (Dekker, New York, 1988), p. 323.